POLITECNICO DI TORINO
Repository ISTITUZIONALE

Moment-Matching-Based Identification of Wave Energy Converters: the ISWEC Device

(Article begins on next page)

12 September 2024

Moment-Matching-Based Identification of Wave Energy Converters: the ISWEC Device [★]

Nicolás Faedo [∗] **Yerai Peña-Sanchez** [∗] **John V. Ringwood** [∗]

[∗] *Centre for Ocean Energy Research, Maynooth University, Maynooth, Ireland (e-mail: nicolas.faedo@mu.ie)*

Abstract The motion of a Wave Energy Converter (WEC) can be described in terms of a particular integro-differential equation, which involves a convolution product accounting for the radiation forces. This convolution term has a computational and a representational drawback both for simulation, and for analysis/design of control strategies. This study presents an application case of a method to obtain a parametric model of the force-to-motion dynamics and/or the radiation force convolution term, based on recent advances in moment-matching. This allows the computation of a model that exactly matches the frequency response of the original system at a chosen set of frequencies, while enforcing specific physical properties of the device.

Keywords: Radiation forces, System identification, Wave energy, Moment-matching

1. INTRODUCTION

Boundary Element Methods (BEM) are commonly used to calculate the hydrodynamic parameters of wave energy converters and, more generally, of various marine structures (Penalba et al., 2017). However, one of the major drawbacks of BEMs is that the results are computed in the frequency-domain and, hence, can only characterise the steady-state motion of the WEC under analysis.

A more comprehensive dynamic modelling approach can be considered, using a time-domain representation of the motion of a WEC, in terms of the well-known Cummins' equation (Cummins, 1962). Moreover, a direct relationship between Cummins' equation and the hydrodynamic frequency-domain data is given in (Ogilvie, 1964) (see Section 3 for further details). The resulting time-domain dynamical model is an integro-differential equation, which contains a convolution term accounting for the fluid memory effects associated with radiation forces acting on a body. Such a convolution operation usually represents a computational drawback, for both simulation and model-based control design.

As discussed in (Faedo et al., 2018), there are several methods which attempt to represent the convolution term of Cummins' equation using a suitable state-space approximation. Two of the most popular methods are those described in (Pérez and Fossen, 2008) (NTNU method) and (Duclos et al., 2001; De Prony, 1795) (Prony's method). The first method uses the frequency-domain data obtained from BEM solvers, while the second one requires the radiation force impulse response to perform such a parametric approximation.

Recently, an approximation technique for the radiation convolution operation and the complete force-to-motion dynamics of a WEC, based on recent advances in model order reduction by moment-matching, has been proposed in (Faedo et al., 2018). Moment-matching methods are based on the idea of interpolating a certain number of points on the complex plane, termed *moments*. A model reduced via moment-matching is such that its transfer function matches the behaviour of the transfer function of the target system at specific interpolation points (i.e. the moments). This allow the design of an approximating model to *exactly* match the frequency response of the device under analysis, at a set of specific key frequencies. This intuitive property allows the enforcement of essential physical characteristics of the device on the reduced model, such as input-output stability. This paper presents the application of this moment-matching-based approach to identify a finite order parametric model of both the force-to-motion dynamics and the radiation force convolution for the full-scale ISWEC (Inertial Sea Wave Energy Converter) device (Bracco et al., 2011). Additionally, a brief comparison with well-known existing methods is provided.

1.1 Notation

$\mathbb{R}^+$ ($\mathbb{R}^-$) denotes the set of non-negative (non-positive) real numbers. $\mathbb{C}^0$ denotes the set of pure-imaginary complex numbers and $\mathbb{C}^-$ denotes the set of complex numbers with a negative real part. The symbol 0 stands for any zero element, with dimension according to the context. The symbol $\mathbb{I}_n$ denotes a size n identity matrix. The spectrum of a matrix $A \in \mathbb{R}^{n \times n}$, i.e. the set of its eigenvalues, is denoted $\sigma(A)$. The symbol $\bigoplus$ denotes the direct sum of n matrices, i.e. $\bigoplus_{i=1}^{n} A_i = \text{diag}(A_1, A_2, \ldots, A_n)$. The notation $\Re\{z\}$ and $\Im\{z\}$, with $z \in \mathbb{C}$, stands for the *real-part* and the *imaginary-part* operators, respectively. The expression $\|x\|_2$, with $x \in \mathbb{C}^{n \times 1}$, denotes the ℓ^2-norm of

the complex-valued vector x. The *Kronecker product* between two matrices $M_1 \in \mathbb{R}^{n \times m}$ and $M_2 \in \mathbb{R}^{p \times q}$ is denoted as $M_1 \otimes M_2 \in \mathbb{R}^{np \times mq}$ while the convolution between two functions $f(t)$ and $g(t)$ over a finite range $[0,t]$, i.e. $\int_0^t f(\tau)g(t-\tau)d\tau$ is denoted $f * g$. The Fourier transform of a function $f(t) \in L^2(\mathbb{R})$ is denoted $\mathscr{F}\{f(t)\} \equiv \hat{f}(t)$, where $L^2(\mathbb{R})$ is the function space of all real-valued square-integrable functions. Finally, the symbol $\varepsilon_n \in \mathbb{R}^{n \times 1}$ denotes a vector with odd components equal to 1 and even components equal to 0.

In the remainder of this section the formal definition of the *Kronecker sum* is provided, since its definition in the literature can be often ambiguous.

Definition 1. (Brewer, 1978) The *Kronecker sum* between two matrices P_1 and P_2, with $P_1 \in \mathbb{R}^{n \times n}$ and $P_2 \in \mathbb{R}^{k \times k}$, is defined (and denoted) as

$$P_1 \hat{\oplus} P_2 \triangleq P_1 \otimes \mathbb{I}_k + \mathbb{I}_n \otimes P_2. \tag{1}$$

2. MOMENT-BASED THEORY

Linear moment-based theory is recalled and summarised in this section (the reader is referred to key studies, such as (Astolfi, 2010)).

Consider a finite-dimensional, single-input, single-output, continuous-time system described, for $t \geq 0$, by the state-space model

$$\dot{x}(t) = Ax(t) + Bu(t), \quad y(t) = Cx(t), \tag{2}$$

where $x(t) \in \mathbb{R}^n$, $u(t) \in \mathbb{R}$, $y(t) \in \mathbb{R}$, $A \in \mathbb{R}^{n \times n}$, $B \in \mathbb{R}^{n \times 1}$ and $C \in \mathbb{R}^{1 \times n}$. Consider the associated transfer function

$$W(s) = C(s\mathbb{I}_n - A)^{-1}B \tag{3}$$

and assume that (2) is minimal (i.e controllable and observable).

Definition 2. (Antoulas, 2005) The 0-moment of system (2) at $s_i \in \mathbb{C}\backslash\sigma(A)$ is the complex number $\eta_0(s_i) = C(s_i\mathbb{I}_n - A)^{-1}B$. The k-moment of system (2) at $s_i \in \mathbb{C}$ is the complex number

$$\eta_k(s_i) = \frac{(-1)^k}{k!}\left[\frac{d^k W(s)}{ds^k}\right]_{s=s_i}, \tag{4}$$

with $k \geq 1$ integer.

In (Astolfi, 2010), a novel interpretation of moments is given in terms of the steady-state response (provided it exists) of the output of the interconnection between a signal generator and system (2). This result is recalled in the following theorem.

Theorem 1. (Astolfi, 2010; Scarciotti and Astolfi, 2017) Consider system (2) and the signal generator

$$\dot{\xi}(t) = S\xi(t), \quad u(t) = L\xi(t), \tag{5}$$

with $\xi(t) \in \mathbb{R}^{\nu \times 1}$, $S \in \mathbb{R}^{\nu \times \nu}$, $L \in \mathbb{R}^{1 \times \nu}$ and $\xi(0) \in \mathbb{R}^{\nu \times 1}$. Assuming that the triple $(L, S, \xi(0))$ is minimal, $\sigma(A) \subset \mathbb{C}^-$, $\sigma(S) \subset \mathbb{C}^0$ and the eigenvalues of S are simple. Let $\Pi \in \mathbb{R}^{n \times \nu}$ be the (unique) solution of the Sylvester equation

$$A\Pi + BL = \Pi S. \tag{6}$$

Then there exists a one-to-one relation between the moments $\eta_0(s_1)$, $\eta_0(s_2)$, $\ldots$, $\eta_0(s_\nu)$, with $s_i \in \sigma(S)$ for all $i = 1, \ldots, \nu$, and the steady-state response $C\Pi\xi$ of the output y of the interconnection of system (2) with the

signal generator (5). In fact, the moments are uniquely determined by the matrix $C\Pi$.

Remark 2. As discussed in (Scarciotti and Astolfi, 2017), the assumption on the eigenvalues of S is a sensible hypothesis, since any contribution from a stable mode will decay exponentially to zero.

Remark 3. From now on, the matrix $C\Pi \equiv \bar{Y}$ is referred as the moment-domain equivalent of $y(t)$.

Lastly, the following key result is recalled from (Astolfi, 2010).

Theorem 4. (Astolfi, 2010) The family of systems described by

$$\dot{\Theta}(t) = (S - GL)\Theta(t) + Gu(t), \quad \theta(t) = \bar{Y}\Theta(t), \tag{7}$$

parametrised on $G \in \mathbb{R}^{\nu \times 1}$, such as $\sigma(S - GL) \cap \sigma(S) = \emptyset$, contains all the models of dimension ν interpolating the moments of system (2) at $\sigma(S)$.

Remark 5. The transfer function of the reduced order model (7) interpolates the transfer function of system (2) at the eigenvalues of S.

Remark 6. The matrix G can be selected to enforce specific properties of the original system on the reduced order model, such as a set of prescribed eigenvalues, as detailed in (Astolfi, 2010) and considered in Section 4.1.

3. WEC EQUATION OF MOTION

A 1-DoF (degree of freedom) WEC is considered in this study, since the extension of the algorithm to multiple degrees of freedom can be done in an analogous procedure.

3.1 Time-domain formulation

The linearised equation of motion for a 1-DoF device can be expressed, in the time-domain, in terms of Newton's second law, as follows:

$$m\ddot{x}(t) = \mathcal{F}_r(t) + \mathcal{F}_h(t) + \mathcal{F}_e(t), \tag{8}$$

where m is the mass of the buoy, $x(t)$ the device excursion, $\mathcal{F}_e(t)$ the wave excitation force, $\mathcal{F}_h(t)$ the hydrostatic restoring force and $\mathcal{F}_r(t)$ the radiation force. The linearised hydrostatic force can be written as $\mathcal{F}_h(t) = -s_h x(t)$, where $s_h > 0$ denotes the hydrostatic stiffness. The radiation force $\mathcal{F}_r(t)$ is modelled based on linear potential theory and, using the well-known Cummins' equation (Cummins, 1962), is

$$\mathcal{F}_r(t) = -\mu_\infty\ddot{x}(t) - \int_0^{+\infty} k(\tau)\dot{x}(t-\tau)d\tau, \tag{9}$$

where $\mu_\infty = \lim_{\omega \to +\infty} A(\omega)$, $\mu_\infty > 0$ represents the added-mass at infinite frequency, $A(\omega)$ is the radiation added mass and $k(t) \in L^2(\mathbb{R})$ is the (causal) radiation impulse response, containing the memory effect of the fluid response. Finally, the linearised equation of motion of the WEC is given by

$$(m + \mu_\infty)\ddot{x}(t) + k(t) * \dot{x}(t) + s_h x(t) = \mathcal{F}_e(t), \tag{10}$$

The internal stability of equation (10), for the WEC case, has been analysed and guaranteed for any physically meaningful values of the parameters and the convolution kernel $k(t)$ involved (Falnes, 2002).

3.2 Frequency-domain formulation

Applying the Fourier transform to (10), and considering velocity as the measurable output, the following representation

$$\hat{x}(j\omega) = \mathcal{F}_e(j\omega)H(j\omega), \qquad (11)$$

where $H(j\omega)$ represents the force-to-velocity frequency response, holds. $H(j\omega)$ is a function of a specific set of characteristic frequency-dependent parameters, namely

$$H(j\omega) = \frac{1}{B(\omega) + j\omega\left[A(\omega) + m\right] + \frac{s_h}{j\omega}}, \qquad (12)$$

where $B(\omega)$ and $A(\omega)$ are the radiation damping and radiation added-mass of the device, respectively (Falnes, 2002). The hydrodynamic parameters $A(\omega)$ and $B(\omega)$ can be efficiently obtained using existing BEM solvers, such as WAMIT or NEMOH.

3.3 Ogilvie's relations: mapping between time and frequency

Francis Ogilvie (Ogilvie, 1964) established a direct relationship between time-domain (10) and frequency-domain (11) models, as a function of the parameters $B(\omega)$ and $A(\omega)$, and the radiation kernel $k(t)$, considering the definition of the Fourier transform, namely

$$
\begin{aligned}
B(\omega) &= \int_0^{+\infty} k(t)\cos(\omega t)dt, \\
A(\omega) &= \mu_\infty - \frac{1}{\omega}\int_0^{+\infty} k(t)\sin(\omega t)dt.
\end{aligned}
\qquad (13)
$$

It follows that the impulse response $k(t)$ can be written as a mapping involving the frequency-dependent parameters as

$$k(t) = \frac{2}{\pi}\int_0^{+\infty} B(\omega)\cos(\omega t)d\omega. \qquad (14)$$

Equation (14) allows a frequency-domain analysis of $k(t)$: a direct application of the Fourier transform, yields

$$\hat{k}(j\omega) = B(\omega) + j\omega\left[A(\omega) - \mu_\infty\right] \equiv K(j\omega). \qquad (15)$$

4. MOMENT-BASED WEC FORMULATION

The equation of motion presented in (10) needs to be re-written in a more suitable structure, since the theory presented in Section 2 is based on a state-space representation of the system under analysis, i.e.

$$\dot{\varphi}(t) = A_\varphi \varphi(t) + B_\varphi \mathfrak{u}(t), \quad y_\varphi(t) = C_\varphi \varphi(t), \qquad (16)$$

where $\varphi(t) = [x(t), \dot{x}(t)]^\intercal \in \mathbb{R}^{n\times 1}$, with $n = 2$, is the state-vector of the continuous-time model and $y_\varphi(t) = \dot{x}(t) \in \mathbb{R}$ is the output of the system. The function $\mathfrak{u}(t) \in \mathbb{R}$, assumed to be the input of system (16), is defined as

$$\mathfrak{u}(t) = \mathcal{F}_e(t) - k(t) * \dot{x}(t), \qquad (17)$$

Under this assumption, the matrices in (16) are given by

$$A_\varphi = \begin{bmatrix} 0 & 1 \\ -\dfrac{s_h}{m + \mu_\infty} & 0 \end{bmatrix}, \; B_\varphi = \begin{bmatrix} 0 \\ \dfrac{1}{m + \mu_\infty} \end{bmatrix}, \; C_\varphi = [0 \; 1]. \qquad (18)$$

Within the moment-based framework, the input $\mathcal{F}_e$ is expressed as a signal generator (5), as

$$\dot{\xi}_e(t) = S\,\xi_e(t), \quad \mathcal{F}_e(t) = L_e\,\xi_e(t), \qquad (19)$$

where the dimension of S and L are as in (5), $\xi_e(t) \in \mathbb{R}^{\nu\times 1}$ and, without loss of generality, the initial condition of the signal generator is chosen as $\xi_e(0) = \varepsilon_\nu$. The matrix S can be written in a real block-diagonal form as

$$S = \bigoplus_{p=1}^{f} \begin{bmatrix} 0 & \omega_p \\ -\omega_p & 0 \end{bmatrix}, \qquad (20)$$

where $\nu = 2f$, $f \geq 0$ integer. With this selection of matrices, the assumption on the minimality of the triple $(L, S, \xi_e(0))$ holds as long as the pair (L, S) is observable. Also note that each ω_p represents a desired interpolation point for the model reduction process (see Remark 5). Then, the moments of system (16), driven by the signal generator (19), can be computed by solving a Sylvester equation (see Theorem 2), i.e.

$$A_\varphi \Pi_\varphi + B_\varphi(L_e - \bar{Z}) = \Pi_\varphi S, \qquad (21)$$

where $\Pi_\varphi \in \mathbb{R}^{n\times\nu}$ and $\bar{Z}$ is the moment-domain equivalent of the radiation convolution term. Note that the moment-domain equivalent of the velocity can be simply expressed in terms of the solution of (21) as $\bar{V} = C_\varphi \Pi_\varphi$.

Proposition 7. (Faedo et al., 2018) The moment-domain equivalent of the convolution integral in (9) can be computed as

$$\bar{Z} = \bar{V}\mathscr{R}, \qquad (22)$$

where $\mathscr{R} \in \mathbb{R}^{\nu\times\nu}$ is a block-diagonal matrix defined by

$$\mathscr{R} = \bigoplus_{p=1}^{f} \begin{bmatrix} r_{\omega_p} & -m_{\omega_p} \\ m_{\omega_p} & r_{\omega_p} \end{bmatrix}, \qquad (23)$$

and its entries depend on the coefficients $A(\omega)$ and $B(\omega)$ of the device at each specific frequency induced by the eigenvalues of S, as

$$r_{\omega_p} = B(\omega_p), \quad m_{\omega_p} = -\omega_p\left[A(\omega_p) - \mu_\infty\right]. \qquad (24)$$

With the analytical definition of the moment-domain equivalent of the radiation force convolution term, the following proposition is recalled from (Faedo et al., 2018), which allows (21) to be solved.

Proposition 8. (Faedo et al., 2018) The moment-domain equivalent of the output y_φ of system (16) can be computed as

$$\bar{V} = L_e\Phi_\varphi^{\mathscr{R}}, \qquad (25)$$

where

$$
\begin{aligned}
\Phi_\varphi^{\mathscr{R}} &= \left[\left(\mathbb{I}_\nu + \Phi_\varphi\mathscr{R}^\intercal\right)^{-1}\Phi_\varphi\right]^\intercal, \\
\Phi_\varphi &= (\mathbb{I}_\nu \otimes C_\varphi)\left(S\,\hat{\oplus}\,A_\varphi\right)^{-1}(\mathbb{I}_\nu \otimes -B_\varphi),
\end{aligned}
\qquad (26)
$$

with $\Phi_\varphi^{\mathscr{R}} \in \mathbb{R}^{\nu\times\nu}$ and $\Phi_\varphi \in \mathbb{R}^{n\nu\times n\nu}$.

Proposition 8 shows an explicit analytical expression for the moment-domain equivalent of the output of system (16). Such a result allows the computation of a reduced order model of system (16) using Theorem 4, in a straightforward way. Explicitly:

$$\tilde{\mathcal{H}}_{\sigma(S)} : \begin{cases} \dot{\Theta}_\varphi(t) = (S - G_\varphi L_e)\,\Theta_\varphi(t) + G_\varphi\mathcal{F}_e(t), \\ \theta_\varphi(t) = \bar{V}\,\Theta_\varphi(t), \end{cases} \qquad (27)$$

is the family of reduced order models parametrised in G_φ, interpolating the moments of system (16) at the eigenvalues of S, where $\bar{V} = L_e\Phi_\varphi^{\mathscr{R}}$.

Remark 9. The reduced order model (27) has dimension $\nu = 2f$, where f is the number of interpolation points (frequencies) selected.

Remark 10. The notation $\tilde{\mathcal{H}}_{\sigma(S)}$ refers to an approximated time-domain model of the force-to-velocity dynamics of the device under analysis, by matching the frequencies selected in $\sigma(S)$.

4.1 Eigenvalue assignment

As discussed in Remark 6, the additional degree of freedom provided by G_φ can be exploited to arbitrarily assign the eigenvalues of the reduced order model (27), i.e. given a set of eigenvalues Σ_φ, one can select G_φ such as $\sigma(S - G_\varphi L_e) = \Sigma_\varphi$. In this case, the following procedure is proposed. Define the transfer function (notation adopted from Remark 10):

$$\tilde{H}_{\sigma(S)}(s) = \bar{V} \left[s\mathbb{I}_\nu - (S - G_\varphi L_e) \right]^{-1} G_\varphi. \qquad (28)$$

The frequency-dependent hydrodynamic parameters $A(\omega)$ and $B(\omega)$ are calculated using hydrodynamic codes at a finite number of frequencies $\omega_i \in [\omega_l, \omega_u]$, with a frequency step of $\Delta\omega_i$, where ω_l and ω_u represents the lower and upper bound of the range, respectively. Such a frequency range depends explicitly on the application. Define the complex-valued vectors H_ω, $\tilde{H}_\omega$ as,

$$H_\omega = \begin{bmatrix} H(j\omega_l) \\ H(j(\omega_l + \Delta\omega_i)) \\ \vdots \\ H(j(\omega_u)) \end{bmatrix}, \quad \tilde{H}_\omega = \begin{bmatrix} \tilde{H}_{\sigma(S)}(j\omega_l) \\ \tilde{H}_{\sigma(S)}(j(\omega_l + \Delta\omega_i)) \\ \vdots \\ \tilde{H}_{\sigma(S)}(j(\omega_u)) \end{bmatrix}. \qquad (29)$$

Then, the proposed optimisation procedure, to assign the eigenvalues of the reduced order model $\Sigma_\varphi \subset \mathbb{C}^-$, can be formulated as,

$$\min_{\Sigma_\varphi \subset \mathbb{C}^-} \| H_\omega - \tilde{H}_\omega \|_2^2. \qquad (30)$$

4.2 On the radiation force convolution operation

The radiation convolution term in (9) defines a linear time-invariant system completely characterised by the impulse response function $k(t)$, where the input considered is the velocity of the device $\dot{x}(t)$, i.e.

$$y_k(t) = k(t) * \dot{x}(t). \qquad (31)$$

A reduced order model, by moment-matching, can be obtained using the result on the moment-domain equivalent of such a convolution term, provided in Proposition 7, as developed in the following.

Assume that the velocity $\dot{x}(t)$ of the WEC can be written as a signal generator in implicit form, in a similar fashion that (19), expressed as a set of linear differential equations given by

$$\dot{\xi}_k(t) = S\,\xi_k(t), \quad \dot{x}(t) = L_k\,\xi_k(t), \qquad (32)$$

with $\xi_k(0) = \varepsilon_\nu$ and L_k such as the pair (L_k, S) is observable. Then, recalling Proposition 7, the moment-domain equivalent of the output of (31) can be straightforwardly computed as $\bar{Y}_k = L_k\mathcal{R}$, and a reduced order model of (31) can be obtained by applying Theorem 3. Specifically:

$$\tilde{\mathcal{K}}_{\sigma(S)} : \begin{cases} \dot{\Theta}_k(t) = (S - G_k L_k)\,\Theta_k(t) + G_k\dot{x}(t), \\ \theta_k(t) = \bar{Y}_k\,\Theta_k(t), \end{cases} \qquad (33)$$

is the family of reduced order models parametrised in G_k, interpolating the moments of system (31) at the

eigenvalues of S, where $\bar{Y}_k = L_k\mathcal{R}$. Following Equation (28), the transfer function of the reduced order model (31) can be computed as,

$$\tilde{K}_{\sigma(S)}(s) = \bar{Y}_k \left[s\mathbb{I}_\nu - (S - G_k L_k) \right]^{-1} G_k, \qquad (34)$$

and the complex-valued vectors K_ω and $\tilde{K}_\omega$ are defined as in (29), by considering the frequency response of the radiation convolution kernel $K(j\omega)$ (15) (instead of $H(j\omega)$), and the reduced order model transfer function $\tilde{K}_{\sigma(S)}(s)$ (instead of $\tilde{H}_{\sigma(S)}(s)$). Then, the set of desired eigenvalues Σ_k of system (33), can be assigned using the same optimisation criterion described in Section 4.1, namely,

$$\min_{\Sigma_k \subset \mathbb{C}^-} \| K_\omega - \tilde{K}_\omega \|_2^2. \qquad (35)$$

5. NUMERICAL EXAMPLE: ISWEC

For this case study, the pitch dynamics of the full-scale ISWEC device Bracco et al. (2011) is considered. The resulting coefficients $A(\omega)$ and $B(\omega)$ (obtained using the open-source BEM solver NEMOH) are shown in Figs. 1**a** and 1**b**.
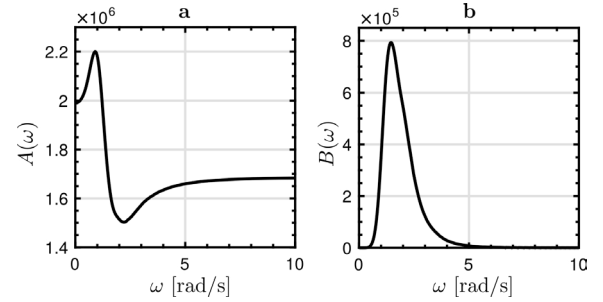
Figure 1. ISWEC pitch characteristics: (**a**) radiation added-mass $A(\omega)$; (**b**) radiation damping $B(\omega)$.

Although the coefficients are computed over a frequency range of $\omega = 0.01$ [rad/s] to $\omega = 10$ [rad/s] (as in Fig.1), a frequency range of $\omega_l = 0.3$ [rad/s] and $\omega_u = 3$ [rad/s] is selected as the key approximation interval (see (Faedo et al., 2018) for further details). For the numerical simulations presented in this paper, the irregular waves are generated from the JONSWAP spectrum (Hasselmann, 1973) shown in Fig.3 (peak period $T_\text{p} = 8$[s], significant wave height $H_\text{s} = 2$[m], peak enhancement factor $\gamma = 3.3$). One can notice that all the non-zero values of the spectrum lie inside the frequency range selected, depicted by a white area in each subsequent plot.
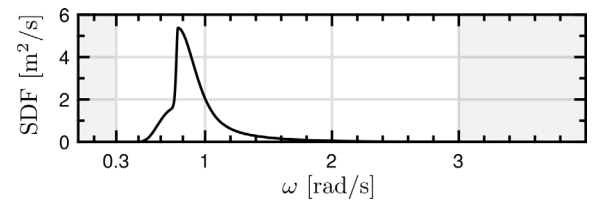
Figure 3. JONSWAP spectrum

5.1 Force-to-velocity case

To compute a parametric model of the force-to-motion frequency response $H(j\omega)$, a suitable set of interpolation

points needs to be chosen, which can be done in a straight-forward manner by inspecting Figs. 1**c** and 1**d**: in the case of a single interpolation point, the resonant frequency of the device ($\omega \approx 1.55[\text{rad/s}]$) represents a sensible choice. As can be appreciated in Fig. 4, the frequency response of the parametric model identified by moment-matching $\tilde{H}_{\{1.55\}}(j\omega)$ (solid-red) and the frequency response of the WEC computed with NEMOH (dashed-black) are in perfect agreement up to graphic accuracy. One can notice that both frequency responses are *exactly* the same (up to any numerical errors) at the interpolation points.
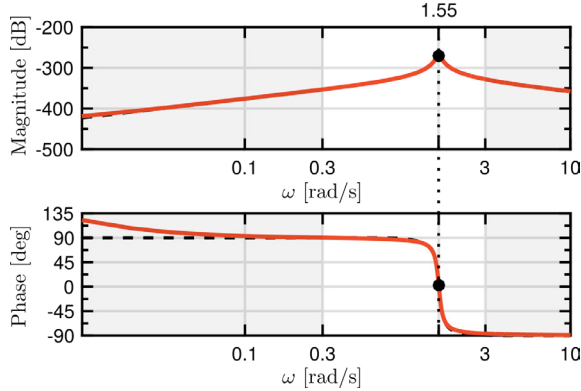

Figure 4. Bode diagram of the force-to-velocity frequency response computed with the coefficients obtained from NEMOH (dashed-black) and the moment-matching parametric model frequency response (solid-red), using a unique interpolation point (black dot).

For the approximation of the ISWEC force-to-motion pitch dynamics, there is no significant improvement when considering more than one interpolation point. However, as discussed in the next section, the approximation error continues decreasing monotonically with increasing parametric model order ν.

5.2 Radiation impulse response case

In an analogous way to the force-to-velocity case, the moment-matching based strategy can be applied to obtain a parametric model of the radiation kernel $K(j\omega)$, as defined in (15). In this case, there is no significant improvement in the approximation accuracy when considering more than two interpolation points, as depicted in Fig. 5.

The parametric model of the radiation kernel response should have particular (physical) properties, as discussed in (Faedo et al., 2018). Some of these properties are recalled in the following: the transfer function $K(s)$ has a zero at the origin, is strictly proper, stable and passive. Fig.6**b** explicitly shows that the first three properties are accomplished for the case of $\tilde{K}_{\{1.45,2.6\}}(s)$. Regarding passivity, Fig. 6**a** shows that the real-part of $\tilde{K}_{\{1.45,2.6\}}(j\omega)$ is always positive which, together with the stability condition, imply that the system is passive. It should be noted that passivity is not explicitly ensured by the approach presented in this paper. However, a non-linear constraint can be added to the optimisation process (35) to systematically guarantee such a property (Faedo et al., 2018), if desired.
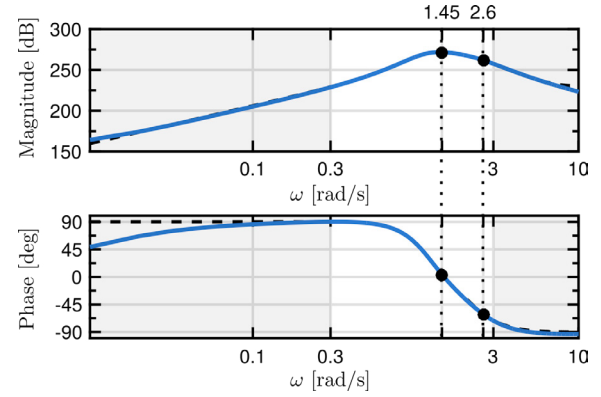

Figure 5. Bode diagram of the radiation kernel frequency response computed with the coefficients obtained from NEMOH (dashed-black) and the moment-matching parametric model frequency response (solid-blue), for three interpolation points (black dots).
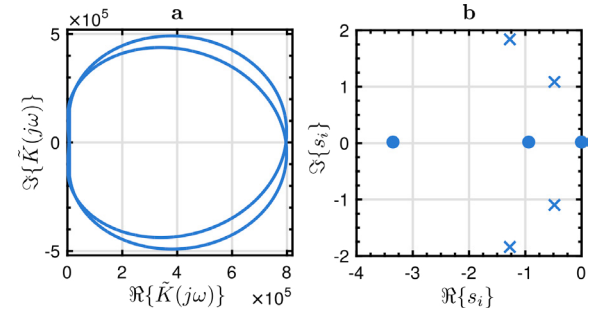

Figure 6. Nyquist diagram (**a**) and pole-zero map (**b**) of $\tilde{K}_{\{1.45,2.6\}}$

Fig.7 depicts the radiation impulse response computed using the data obtained from NEMOH (dotted-black), and the impulse response of the reduced order model $\tilde{\mathcal{K}}_{\{1.45,2.6\}}$ (solid-blue). It can be noted that both impulse responses are almost identical, validating the transient response of the parametric model $\tilde{\mathcal{K}}_{\{1.45,2.6\}}$.

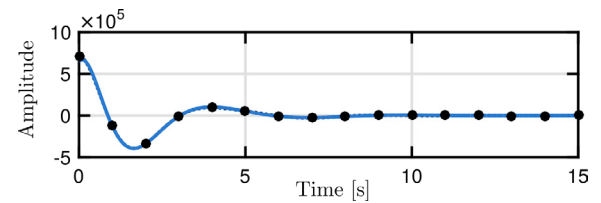Figure 7. Comparison between the radiation impulse response computed with data from NEMOH (dotted-black) and the impulse response of $\tilde{\mathcal{K}}_{\{1.45,2.6\}}$ (solid-blue).

5.3 Comparison with existing strategies

In this subsection, the moment-based strategy presented in this paper is compared to the methods proposed in (Pérez and Fossen, 2008) (NTNU) and (Duclos et al., 2001; De Prony, 1795) (Prony's). The comparison is carried out using time-domain data and the results are given in terms of Normalised Root Mean Square Error (NRMSE) between the steady-state velocity of the WEC and the steady-state

velocity computed using the models identified with each different strategy. Since the irregular waves are generated using random phases, a mean of 20 different simulations is considered to compute each NRMSE in order to obtain representative results, which are shown in Fig. 8.

While NTNU and Prony's methods (as developed in (Pérez and Fossen, 2008) and (De Prony, 1795), respectively), only provide a parametric model of the radiation force convolution term of (10), the moment-matching strategy presented in this study can be used to obtain a parametric model of both the radiation force convolution term and the force-to-motion dynamics directly. It should be noted that, if the radiation convolution term is approximated, two additional elements are required in the state-space approximation to compute the force-to-motion simulation (position and velocity). Therefore, and as can be appreciated in Fig.8, the methods presented which approximate only the radiation force convolution term have a minimum state-space order of 4.
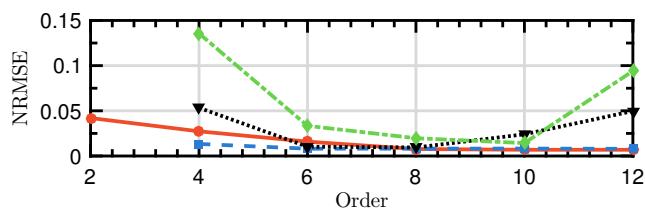

Figure 8. NRMSE for moment-matching force-to-velocity approximated model (solid-red), and the approximated radiation impulse response computed using moment-matching (dashed-blue), NTNU (dotted-black) and Prony's (dash-dot-green) methods for different model orders.

For this case study (and for orders between 6 and 10) all the tested strategies obtain reasonably accurate approximations (NMRSE < 5%). One can notice that, among the selected strategies, only the moment-matching method achieve a *monotonically decreasing* NRMSE.

6. CONCLUSIONS

This paper shows how to obtain a finite order parametric model from frequency-domain data for both the force-to-motion and the radiation convolution term of Cummins' equation for the case of the ISWEC device, using a recent strategy based on model order reduction by moment-matching. By considering this strategy, it can be ensured that the identified parametric models *exactly* match the behaviour of the system at a set of key frequencies while enforcing, at the same time, specific physical properties in the model.

The results obtained with this moment-matching strategy are compared with well-established algorithms in the wave energy community. It is demonstrated that only the approximation error obtained by the moment-matching strategy decreases monotonically when increasing the model order. In addition, only the radiation impulse response approximating model computed based on moment-matching fulfills the radiation force system (physical) properties.

Finally, an open-source MATLAB toolbox, to obtain finite-order hydrodynamic models using this moment-matching strategy, is currently under development and it will be available over the next months at the Centre for Ocean Energy Research website[1].

REFERENCES

Antoulas, A.C. (2005). *Approximation of large-scale dynamical systems.* SIAM.

Astolfi, A. (2010). Model reduction by moment matching for linear and nonlinear systems. *IEEE Transactions on Automatic Control*, 55(10), 2321–2336.

Bracco, G., Giorcelli, E., and Mattiazzo, G. (2011). Iswec: a gyroscopic mechanism for wave power exploitation. *Mechanism and machine theory*, 46(10), 1411–1424.

Brewer, J. (1978). Kronecker products and matrix calculus in system theory. *IEEE Transactions on circuits and systems*, 25(9), 772–781.

Cummins, W. (1962). The impulse response function and ship motions. Technical report, DTIC Document.

De Prony, B.G.R. (1795). Essai éxperimental et analytique: sur les lois de la dilatabilité de fluides élastique et sur celles de la force expansive de la vapeur de lalkool,a différentes températures. *Journal de lécole polytechnique*, 1(22), 24–76.

Duclos, G., Clément, A.H., Chatry, G., et al. (2001). Absorption of outgoing waves in a numerical wave tank using a self-adaptive boundary condition. *International Journal of Offshore and Polar Engineering*, 11(03).

Faedo, N., Peña-Sanchez, Y., and Ringwood, J.V. (2018). Finite-order hydrodynamic model determination for wave energy applications using moment-matching. *Ocean Engineering*, 163, 251–263.

Falnes, J. (2002). *Ocean waves and oscillating systems: linear interactions including wave-energy extraction.* Cambridge university press.

Hasselmann, K. (1973). Measurements of wind wave growth and swell decay during the Joint North Sea Wave Project (JONSWAP). *Dtsch. Hydrogr. Z.*, 8, 95.

Ogilvie, T.F. (1964). Recent progress toward the understanding and prediction of ship motions. In *5th Symposium on naval hydrodynamics*, volume 1, 2–5. Bergen, Norway.

Penalba, M., Kelly, T., and Ringwood, J.V. (2017). Using NEMOH for modelling wave energy converters: A comparative study with WAMIT.

Pérez, T. and Fossen, T.I. (2008). Time-vs. frequency-domain identification of parametric radiation force models for marine structures at zero speed. *Modeling, Identification and Control*, 29(1), 1–19.

Scarciotti, G. and Astolfi, A. (2017). Data-driven model reduction by moment matching for linear and nonlinear systems. *Automatica*, 79, 340–351.

[1] http://www.eeng.nuim.ie/coer/